ELECTRONS AND IONS IN A RADIO-FREQUENCY OXYGEN PLASMA

W.W. Stoffels, E. Stoffels, D. Vender, G.M.W. Kroesen and F.J. de Hoog,
Department of Physics, Eindhoven University of Technology,
P.O. Box 513, 5600 MB Eindhoven, The Netherlands.

Abstract

Measurements of the electron and negative ion densities in a 13.56 MHz capacitively coupled oxygen plasma are performed by means of a microwave resonance technique in combination with photodetachment. A kinetic model is developed incorporating volume and wall reactions of ions as well as neutrals. It is shown by matching the experimental results with the model that the dominant ion is O^- (density: 5×10^{15} m^{-3}), whereas the O_2^- and O_3^- densities reach 10 to 20% of the total negative ion density. The ratio of negative ion to electron density varies between 5 and 10 and decreases with pressure and rf power. The influence of neutral chemistry on the negative ion density is demonstrated. Spatial distribution of ions is pressure dependent: at low pressure a parabolic profile has been found, which is independent of discharge chemistry.

Introduction

Oxygen plasmas are widely used for industrial material processing, due to their ability to clean, oxidize, etch and ash samples without heating them to high temperatures. Applications include dry etching of photoresist, polymer and biological materials, formation of oxide films and ashing for pretreatment of specimens in chemical analysis. Furthermore, some oxygen discharges are efficient sources of ozone, atomic oxygen and a variety of excited species. In this work a low pressure radio-frequency (rf) oxygen discharge is treated.

A global kinetic model of the discharge has been developed in order to explain the experimentally observed negative ion densities. The model facilitates comparisons of the importance of several elementary processes involving negative ions, such as ion-ion recombination and associative detachment. Table I gives an overview of the reactions incorporated into the model. The input parameters for the calculations are pressure, gas flow and the experimentally determined electron density. As the latter changes with the input power, a complete set of experimental variables (pressure, gas flow and power input) is introduced into the model. Some of the rate constants (10,12) used in the calculations are modified and estimates are made for sticking coefficients of various species [1]. In our

Table I: Overview of the reactions in the kinetic model, with the rate constants for $T_e = 3$ eV, $T_g = 300$ K. D is the diffusion coefficient, H the height of the cavity and γ the sticking probability. The pressure p is in Torr and the flow $\mathcal{F}$ in sccm. A complete list of references is given in [1]. In the text the reactions are referred to by their number from the table enclosed in brackets.

Reaction				**Rate constant [m^3s^{-1}] or frequency [s^{-1}]**
Neutrals:				
(1)	$O_2 + e$	$\rightarrow$	$2O + e$	2.4×10^{-15}
(2)	$O_2(a) + e$	$\rightarrow$	$2O + e$	$k_1 \exp(0.99/T_e)$
(3)	$O_2 + e$	$\rightarrow$	$O_2(a) + e$	6.1×10^{-16}
(4)	$O_2(a) + e$	$\rightarrow$	$O_2 + e$	$(3/2)k_3 \exp(0.99/T_e)$
(5)	$O_3 + e$	$\rightarrow$	$O + O_2 + e$	$5 \times k_1$
O^-:				
(6)	$O_2 + e$	$\rightarrow$	$O^- + O$	3.5×10^{-17}
(7)	$O_2(a) + e$	$\rightarrow$	$O^- + O$	1.2×10^{-16}
(8)	$O^- + O_2^+$	$\rightarrow$	neutrals	10^{-13}
(9)	$O^- + O$	$\rightarrow$	$O_2 + e$	1.4×10^{-16}
(10)	$O^- + O_2(a)$	$\rightarrow$	$O_3 + e$	10^{-16}
(11)	$O^- + e$	$\rightarrow$	$O + 2e$	2.4×10^{-14}
O_2^-:				
(12)	$O^- + O_2(a)$	$\rightarrow$	$O + O_2^-$	3.3×10^{-17}
(13)	$O_3 + e$	$\rightarrow$	$O_2^- + O$	10^{-15}
(14)	$O_2^- + O_2^+$	$\rightarrow$	neutrals	10^{-13}
(15)	$O_2^- + O$	$\rightarrow$	$O_3 + e$	1.5×10^{-16}
(16)	$O_2^- + O$	$\rightarrow$	$O_2 + O^-$	3.3×10^{-16}
(17)	$O_2^- + O_2(a)$	$\rightarrow$	$2O_2 + e$	2×10^{-16}
O_3^-:				
(18)	$O^- + O_3$	$\rightarrow$	$O + O_3^-$	5.6×10^{-16}
(19)	$O_3^- + O_2^+$	$\rightarrow$	neutrals	10^{-13}
(20)	$O_3^- + O$	$\rightarrow$	$O_2^- + O_2$	3.2×10^{-16}
(21)	$O_3^- + O$	$\rightarrow$	$2O_2 + e$	3×10^{-16}
Wall processes:				$\nu = D/\Lambda_{\text{eff}}^2$
(22)	$O + O_{wall}$	$\rightarrow$	O_2	$D = 2.05 \times 10^{-2} p^{-1}, \gamma = 0.5$
(23)	$O + O_{wall}$	$\rightarrow$	$O_2(a)$	0
(24)	$O_2(a)$	$\rightarrow$	O_2	$\gamma = 0$
Flow loss:				
(25)	for O, $O_2(a)$, O_3			$0.01 \times \mathcal{F}/p$

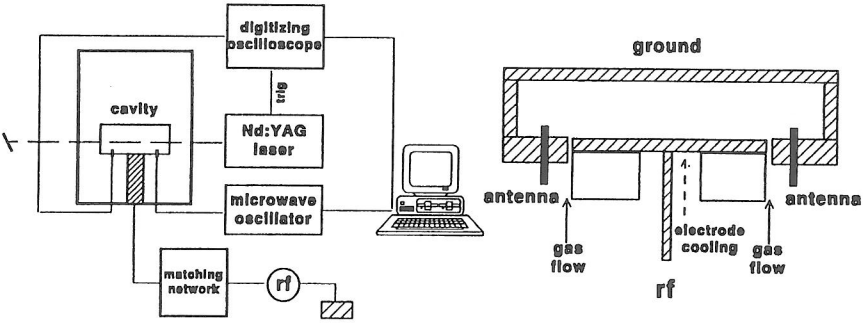

Figure 1: Left: a schematic view of the experimental setup, right: the cavity configuration.

model the positive ion density is obtained from the charge neutrality condition and not from the positive ion balance equation. As the positive ion and electron densities are known, these data can be used to determine the electron ionization temperature.

Experimental

The measurements have been carried out in a 13.56 MHz capacitively coupled plasma confined in an aluminum cylinder with a diameter of 17.5 cm and a height of 5 cm (see Fig. 1). The lower rf electrode is water cooled and has a diameter of 12 cm. Typical discharge parameters are 5 to 500 mTorr, 10 W and 30 sccm. A detailed description of the setup as well as the measurement technique is given elsewhere [1, 2].

In order to measure the electron density a microwave resonance method has been used in which the cylinder containing the plasma serves as a cavity. As the resonance frequency of the cavity (about 3 GHz) is determined by the free electron density inside, this provides an accurate method to determine the space averaged electron density. Models and measurements of electronegative plasmas however have shown that the electron density profile is flat in the whole plasma glow and a sharp decrease is found in the space charge region towards the electrodes [3, 4]. The microwave resonance method can be modified to obtain the negative ion density. A pulsed Nd:YAG laser (pulse width - 10 ns) is used to photodetach electrons from the negative ions and the additional shift in the resonance frequency, caused

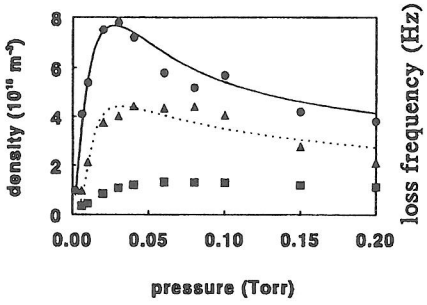

Figure 2: The measured and calculated ($T_e = 3$ eV) total space averaged negative ion density (dots, solid line), the O_2^- density ($\times 5$, triangles, dotted line) and the measured electron density (squares) as a function of pressure at 10 W and 30 sccm.

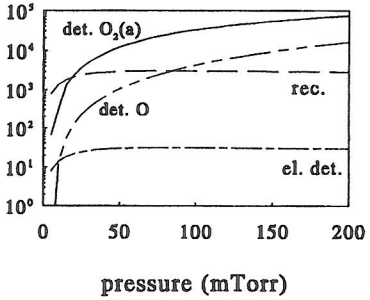

Figure 3: Loss frequencies for negative ions in an oxygen rf plasma as a function of pressure due to detachment by O_2(a) (solid), O (dash-dot-dot), recombination (dashed) and electron detachment (dash-dot).

by the detached electrons, is measured. The spatial ion distribution can be determined with a resolution of 1 mm. The photodetachment technique allows selective detection of various negative ions (with different detachment energies E_a) by choosing an appropriate laser photon energy. In case of an oxygen plasma the most important ions are O^- ($E_a = 1.46$ eV), O_2^- (0.44 eV) and O_3^- (2.10 eV). Using the fundamental frequency of the Nd:YAG laser ($\lambda = 1064$ nm, 1.16 eV) it is possible to separate O_2^- from the other ions. A sketch of the complete experimental setup for the density measurements is shown in Fig. 1.

Results and discussion

The measured electron and ion densities as a function of pressure are shown in Fig. 2. The ratio of the total negative ion to electron density is about 5 to 10 and decreases with pressure. The dominant negative ion is O^-, whereas the molecular ions form about 10-20% of the total density. The model in which the previously estimated sticking coefficients [1] and reaction constants are incorporated describes the pressure dependencies of ion densities very well. In Fig. 3 the various loss frequencies for negative ions in the plasma are plotted as a function of pressure. The competition between ion-ion recombination (8) and neutral

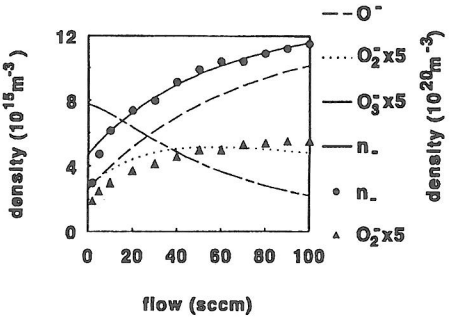

Figure 4: Measured and calculated negative ion densities as a function of the gas flow at 25 mTorr and 10 W. Total negative ion density: dots and solid line; O^- density: dashed line; O_2^- density: triangles and dotted line; O_3^- density: dash-dotted line.

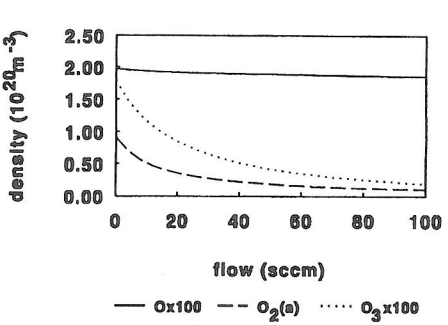

Figure 5: Calculated densities of $O_2(a)$ (dashed line), O (solid line), and O_3 (dotted line) as a function of gas flow. The pressure is 25 mTorr and the power 10 W. The O and O_3 densities are shown enlarged100 times.

detachment (9,10) explains the observed negative ion density. At low pressures the O^- balance is governed by dissociative attachment to O_2 (6) and ion-ion recombination (8), which causes the O^- density to increase as the square root of pressure. The densities of the detaching species (O_2(a) and O) increase with pressure as p or p^2 [1]. Therefore neutral detachment (9,10) becomes dominant at pressures above 30 mTorr. As a result the negative ion density reaches a maximum at 30 mTorr. The behavior of O_2^- and O_3^- can be explained in a similar way as has been done for O^-. Since the molecular ions are formed mainly by charge exchange between O^- and $O_2(a)$ or O_3 (12,18) and destroyed again by recombination and detachment, their dependencies on pressure are similar.

The electron density does not change with the gas flow rate. As the neutral chemistry (mainly O_2(a)) influences the negative ion density, there is a gas flow rate effect on the negative ion density. The flow dependence of the negative ion densities is compared to the model in Fig. 4 for a pressure of 25 mTorr; the calculated neutral densities are shown in Fig. 5. A small discrepancy occurs between the measured and calculated negative ion densities at at very low flow rates ($\leq$ 10 sccm). This is attributed to a changing wall condition (heating), which influences the production of O_2(a) (23). This effect is treated in detail in [1].

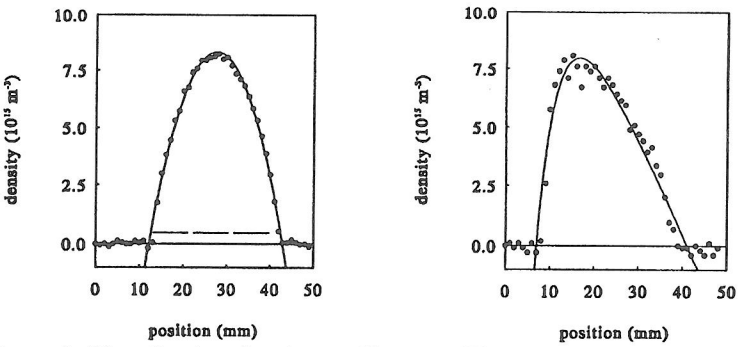

Figure 6: Negative ion density profile at 10 W, 30 sccm. Left: at 10 mTorr, right: at 100 mTorr. The electron density is indicated by the dashed line.

Fig. 6 shows the axial ion density profiles. Since the negative ions are produced and destroyed uniformly in the plasma, the positive ions, which are destroyed by diffusion to the wall, determine the spatial ion distribution. At low pressures the ionization is homogeneous in the plasma glow. Uniform production, balanced by transport to the wall, results in the observed parabolic profile. Such profiles have been found in other gases at low pressures [2, 6]. At higher pressures the ionization rate has a peak at the sheath edge of the powered electrode. As a result, the ion profile is shifted.

References

[1] E. Stoffels, W.W. Stoffels, D. Vender, M. Kando, G.M.W. Kroesen, and F.J. de Hoog. *Phys. Rev. E* 51. 2425, 1995.

[2] E. Stoffels and W.W. Stoffels. *Electrons, ions and dust in a radio-frequency discharge.* Ph.D Thesis, Eindhoven University of Technology, 1994.

[3] J.D.P. Passchier, W.J. Goedheer. *J. Appl. Phys.* 73. 1073, 1993.

[4] M. Haverlag. *Plasma chemistry of fluorocarbon rf discharges used for dry etching.* Ph.D Thesis, Eindhoven University of Technology, 1991.

[5] D. Vender, W.W. Stoffels, E. Stoffels, G.M.W. Kroesen, and F.J. de Hoog. *Phys. Rev. E* 51. 2436, 1995.